Optical illustration of a varied fractional Fourier-transform order and the Radon–Wigner display

David Mendlovic, Rainer G. Dorsch, Adolf W. Lohmann, Zeev Zalevsky, and Carlos Ferreira

Based on an all-optical system, a display of a fractional Fourier transform with many fractional orders is proposed. Because digital image-processing terminology is used, this display is known as the Radon–Wigner transform. It enables new aspects for signal analysis that are related to time- and spatial-frequency analyses. The given approach for producing this display starts with a one-dimensional input signal although the output signal contains two dimensions. The optical setup for obtaining the fractional Fourier transform was adapted to include only fixed free-space propagation distances and variable lenses. With a set of two multifacet composite holograms, the Radon–Wigner display has been demonstrated experimentally.

Key words: Fourier optics, optical information processing, fractional Fourier transforms, Wigner distribution functions, graded-index media, Radon–Wigner display.

1. Introduction

Recently, the fractional Fourier transform (FRT) has become a useful mathematical operation for signal processing. An optical implementation of it was obtained with a graded-index (GRIN) medium.[1–4] In digital image processing and in tomography a similar transformation, adapted to time-frequency operation, has been suggested. This transformation is called the Radon–Wigner transform.[5–7] The relation between the FRT and the Radon–Wigner transform was discussed in Ref. 8. By calculating and displaying the FRT for all possible angles, one obtains a plot that we call the (x, p) display.[9] This display contains a continuous representation of the FRT of a signal as a function of the fractional Fourier order p and as such might obtain complex values. Note that this display is reversible, and one can calculate the original function from it. This display may also be useful in optics because, for example, it shows explicitly the propagation of a signal inside a GRIN medium. Wood and Barry[6] suggested a similar display, which they called the Radon–Wigner display, and showed its application to the detection and classification of linear FM components. However, their display is the intensity representation of the (x, p) display, and thus it is not always reversible. Thresholding the (x, p) display followed by filtered backprojection to the space–frequency plane reduces noise and cross-term power for multicomponent linear FM signals.[7] In this paper an optical implementation of the (x, p) display is suggested.

In Section 2 is a mathematical analysis of the suggested optical setup. In Section 3 the experimental results are illustrated.

2. Mathematical Analysis

The FRT is a mathematical operation that has applications in signal analysis and processing. The integral definitions of the FRT are[3]

$$u_p(x) = C_1 \int_{-\infty}^{\infty} u(x_0) \exp\left[\frac{i\pi}{\lambda f_1 \tan \phi}\,(x_0^2 + x^2)\right] \times \exp\left(\frac{-2\pi i}{\lambda f_1 \sin \phi}\, x x_0\right) dx_0, \qquad (1)$$

$$\phi = p\,\frac{\pi}{2},$$

where p is the fractional order, λ is a wavelength, f_1 is

D. Mendlovic, R. G. Dorsch, and Z. Zalevsky are with the Faculty of Engineering, Tel-Aviv University, 69978 Tel Aviv, Israel. A. W. Lohmann is with the Department of Physics of Complex Systems, Weizmann Institute of Science, 76100 Rehovot, Israel. C. Ferreira is with the Departament Interuniversitari d'Òptica, Faciltat de Física, Universitat de València, C/Doctor Moliner 50, 46100 Burjassot, Valencia, Spain.

Received 20 March 1995; revised manuscript received 21 February 1996.

0003-6935/96/203925-05$10.00/0

a scaling factor of the transformed function, and C_1 is a constant that equals

$$C_1 = \frac{\exp\left\{-i\left[\frac{\pi\ \mathrm{sgn}(\sin\phi)}{4} - \frac{\phi}{2}\right]\right\}}{|\sin\phi|^{1/2}}. \tag{2}$$

Recently the FRT operation was implemented optically. The bulk approach implementation[3] shows that an FRT of order p can be performed with a setup consisting of a lens (with focal length f), a free-space propagation (of distance z), and an additional lens (with focal length f) placed at the output plane. The focal length of the lens f and the distance z should fulfill

$$f = \frac{f_1}{\tan\frac{\phi}{2}}, \qquad z = f_1 \sin\phi = Rf_1. \tag{3}$$

We call a display that contains a continuous representation of the FRT of a signal as a function of the fractional Fourier order the (x, p) display, and it may be useful both for digital signal processing (see Ref. 7) and for optics (e.g., it shows explicitly the propagation of a signal through a GRIN medium). For a one-dimensional (1-D) object this plot contains two axes: the space and the FRT order p. The vertical axis x is the spatial 1-D light distribution $u_p(x)$ of the p-order FRT of the original function $u_0(x)$. The horizontal axis is the FRT order p. More explicitly one can write

$$F(x, p) = u_p(x). \tag{4}$$

As a result, all the fractional Fourier orders of the original function $u_0(x)$ are calculated and displayed in one plot.

We suggest, using a multichannel approach, an optical setup that optically implements the calculations of the (x, p) display. The input 1-D object is converted to a two-dimensional (2-D) object by the use of cylindrical lenses. Then a setup that consists of a sandwich of three phase masks separated by two free-space propagations is constructed. The masks consist of many strips, each one a different channel that performs an FRT with a different order over the input signal. Each strip is a Fresnel zone plate with a different focal length that is selected for obtaining the different fractional order p, and eventually the 2-D output will be exactly the (x, p) display of the 1-D input function. Thus the first step is to prove that the setup illustrated in Fig. 1 indeed provides the FRT with different fractional orders. Note that in this setup we permit changing the focal lengths (the different strips of the mask), but the free-space propagation distances are constant and remain fixed for all the fractional orders.

According to Ref. 10, the optical structure of Fig. 2(a) is totally analogous to the structure of Fig. 2(b)

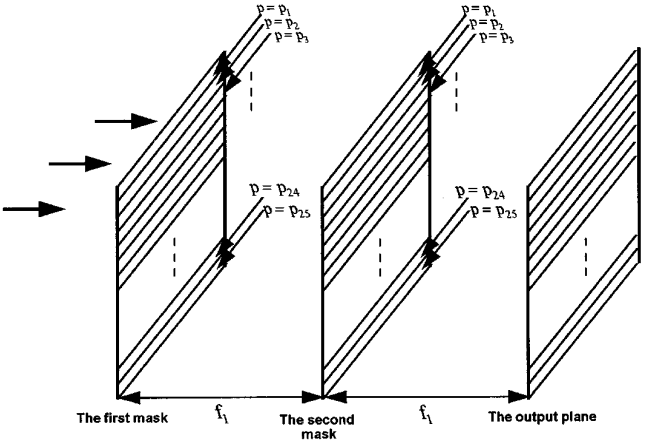

Fig. 1. Suggested optical setup for obtaining the (x, p) display.

for

$$f' = \frac{f_1}{R} = \frac{f_1}{\sin\phi}. \tag{5}$$

The proof is obtained by the use of some of the Wigner optics tools.[10] The tools needed are:

- An inversion, expressed at the Wigner space as

$$u(x) \rightarrow u(-x), \qquad W(x, \xi) \rightarrow W(-x, -\xi), \tag{6}$$

where x and ξ are the two coordinates of the Wigner transform. When matrix terminology is used, the matrix that operates over the

$$\begin{bmatrix} x \\ \xi \end{bmatrix}$$

vector and inverts it

$$\begin{bmatrix} -x \\ -\xi \end{bmatrix}$$

is

$$\begin{bmatrix} -1 & 0 \\ 0 & -1 \end{bmatrix}.$$

This is true because

$$\begin{bmatrix} -1 & 0 \\ 0 & -1 \end{bmatrix}\begin{bmatrix} x \\ \xi \end{bmatrix} = \begin{bmatrix} -x \\ -\xi \end{bmatrix}.$$

- A Fourier transformation, expressed in the Wigner plane with the matrix

$$\begin{bmatrix} 0 & -1 \\ 1 & 0 \end{bmatrix}.$$

- A lens with a focal power of

$$\frac{R}{f_1}\left[\exp\left(-i\pi\frac{x^2R}{\lambda f_1}\right)\right],$$

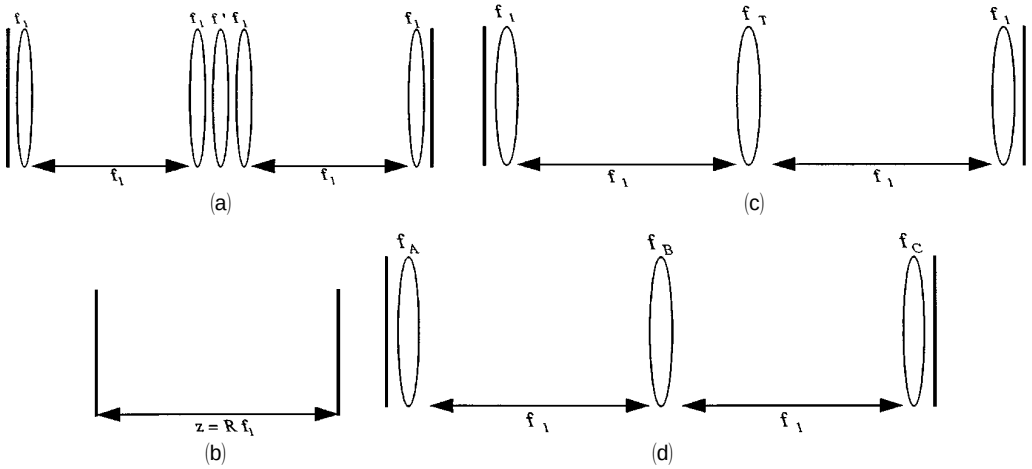

Fig. 2. Optical configurations: (a), and (b) Totally equivalent setups, (c) configuration equivalent to the free-space propagation of distance z, and (d) setup yielding the FRT with constant distances and varying focal lengths.

expressed with the matrix

$$\begin{bmatrix} 1 & 0 \\ R & 1 \end{bmatrix}.$$

- Free-space propagation over a distance of $z = Rf_1$, expressed with the matrix

$$\begin{bmatrix} 1 & -R \\ 0 & 1 \end{bmatrix}.$$

Thus the setup described in Fig. 2(b) can be written as

$$\begin{bmatrix} 0 & -1 \\ 1 & 0 \end{bmatrix}\begin{bmatrix} 1 & 0 \\ R & 1 \end{bmatrix}\begin{bmatrix} 0 & -1 \\ 1 & 0 \end{bmatrix} = \begin{bmatrix} 0 & -R \\ 0 & 1 \end{bmatrix}\begin{bmatrix} -1 & 0 \\ 0 & -1 \end{bmatrix}. \quad (7)$$

Hence a free-space propagation of length $z = Rf_1$ can be represented as the structure illustrated in Fig. 2(c) where

$$f_T = \frac{f_1}{2 + \sin \phi}. \quad (8)$$

Applying this result to the basic FRT setup mentioned above, we replace the free-space propagation part with the setup illustrated in Fig. 2(c). After combining the focal powers of the lenses, one obtains the setup in Fig. 2(d) with

$$f_a = \frac{f_1}{\tan \dfrac{\phi}{2} + 1}, \quad (9)$$

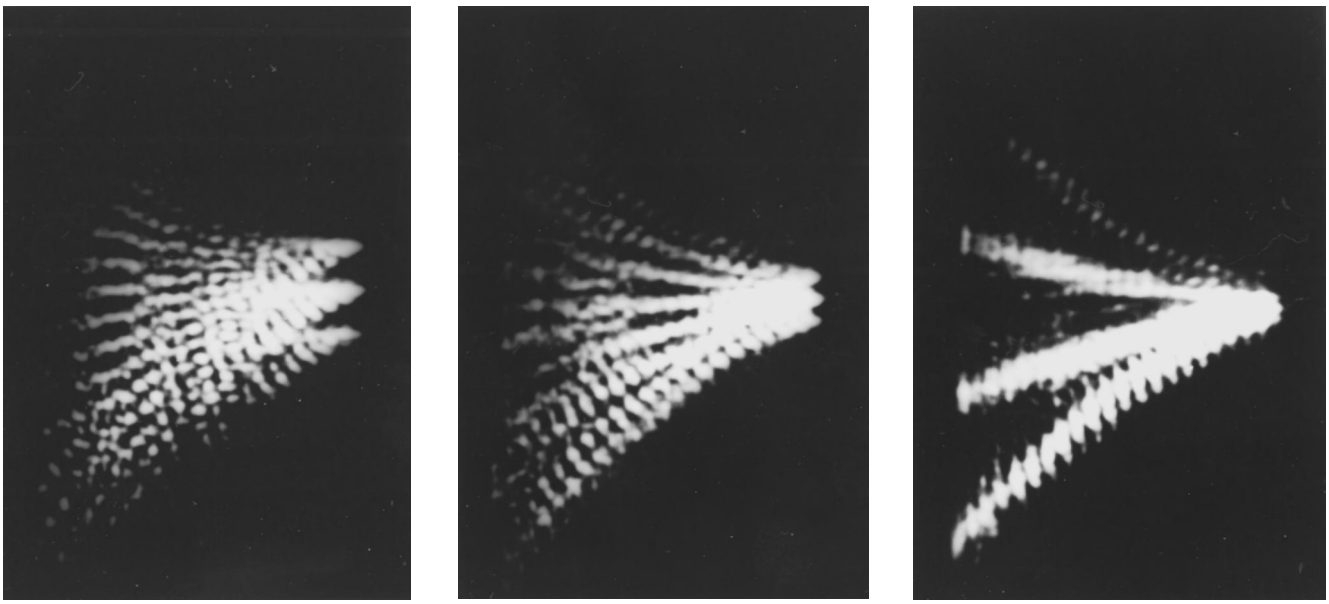

(a) (b) (c)

Fig. 3. Experimental results for the input of a Ronchi grating of (a) 200 lines/cm, (b) 100 lines/cm, and (c) 50 lines/cm.

$$f_b = \frac{f_1}{\sin\phi + 2}, \tag{10}$$

$$f_c = f_a. \tag{11}$$

Thus the setup suggested in Fig. 1 is appropriate for generating the (x, p) display because the distances of free-space propagation f_1 are fixed and because focal lengths f_a, f_b, f_c are varied according to the fractional order p.

Two masks that act as a varied Fresnel zone plate were constructed. These masks were generated in a multifacet (multichannel) manner.[11] Each strip (different channel) in the mask is a Fresnel zone plate with different focal power according to the fractional orders p of the specific strip. The different focal lengths of the different strips in the first mask are related to the fractional order p according to Eq. (9). In the second mask they relate according to Eq. (10). The third mask [with focal lengths according to Eq. (11)] may be placed in the output plane. This mask is necessary only if the field distribution of the output is examined.

The masks' function is

$$t(x, y) = \exp(2\pi i\alpha x)\exp\left(-\pi i\frac{x^2}{\lambda f}\right)\exp\left(-\pi i\frac{y^2}{\lambda Z_R}\right). \tag{12}$$

The generation of the mask was done with computer-generated-interferogram technology[12] that results in a binary mask. The phase term of

$$\exp\left(-\pi i\frac{x^2}{\lambda f}\right)$$

is the encoded Fresnel zone plate; f is f_a, f_b, or f_c (depending on whether this is the first, second, or third mask, respectively), and it varies from one strip to the other as a function of the fractional order as shown in Eqs. (9)–(11). The term $\exp(2\pi i\alpha x)$ is a carrier frequency that diverts the information to the first diffraction order. To avoid overlaps between the different diffraction orders, we require that

$$\max\left|\frac{\partial\theta}{\partial x}\right| < \frac{2\pi\alpha}{2}, \tag{13}$$

where $\theta = \pi x^2/\lambda f$. Thus

$$\alpha > \left|\frac{x_{\max}}{\lambda f_{\min}}\right|, \tag{14}$$

where $x_{\max}$ is the maximal x coordinate and $f_{\min}$ is the minimal focal power. The term

$$\exp\left(-\pi i\frac{y^2}{\lambda Z_R}\right)$$

exists only in the first filter mask. It was added to avoid overlap between the different strips because of diffraction. Note that in the output plane the sizes of the strips will be as in the first mask. This helps avoid interference noise between the different facets. We assumed that the input wave is a Gaussian wave in its waist. Z_R is the Rayleigh distance of the Gaussian wave, and it equals

$$Z_R = \frac{\pi w^2}{2\lambda}, \tag{15}$$

where w is the waist width. Because the distance between the first and the second mask is f_1, we wish that $Z_R = f_1$.

3. Experimental Results

The setup suggested in Fig. 1 was constructed. The prepared masks were designed to be a size of 10 mm

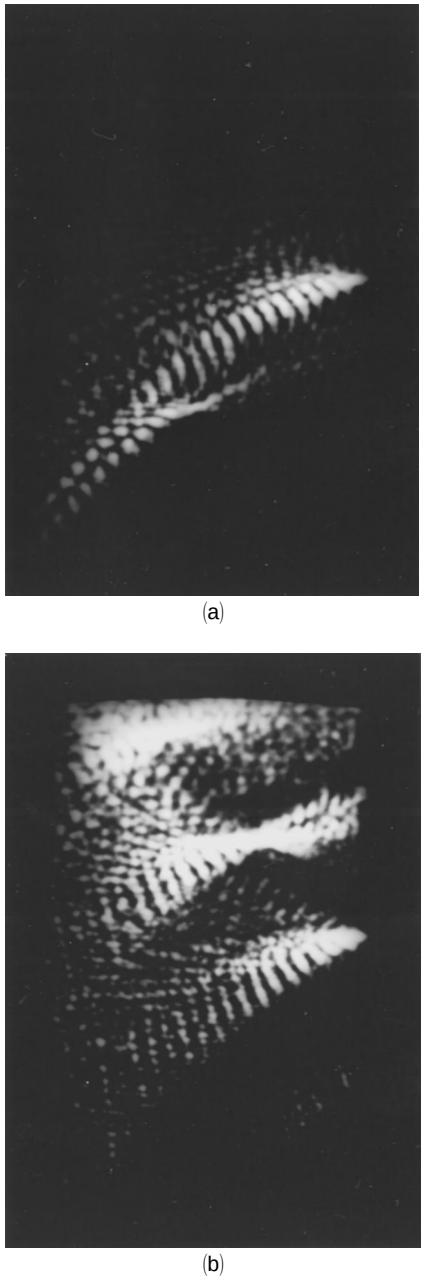

(a)

(b)

Fig. 4. Experimental results of the input of a chirp with the constants (a) 1.5 m, and (b) 2.5 m.

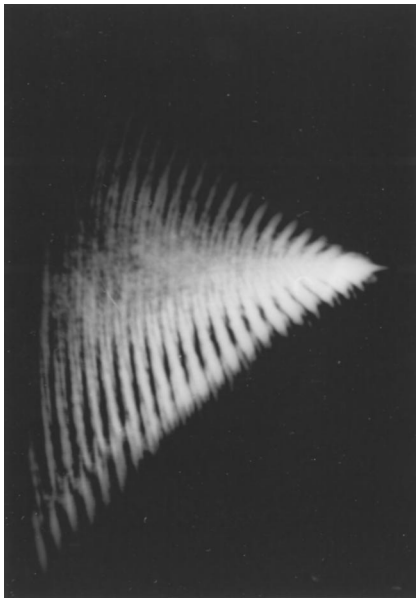

Fig. 5. Experimental results of the input of a plane wave.

$\times$ 10 mm with $\lambda = 532$ nm. The number of strips (channels) was 25; thus, because we assumed that the input wave was at its waist, $w = 10\ \text{mm}/25 = 0.4$ mm, the width of the beam at the second mask is $w/\sqrt{2}$; i.e., only $1/\sqrt{2}$ of each strip is illuminated. According to $w = 0.4$ mm one obtains $Z_R = 472$ mm. Because in practice the input wave is not exactly at its waist, the real free-space propagation distance should be a little smaller than 472 mm; thus we chose the free-space propagation distance f_1 to be 450 mm. Because the masks' sizes are 10 mm $\times$ 10 mm, $x_{\max} = 5$ mm. For the first mask $f_{a_{\min}}$ (obtained for $p = 1$) is $f_1/2 = 225$ mm; thus, according to Eq. (14), α should be greater than 42. We chose $\alpha = 60$. For the second mask the minimal power length obtained for $p = 1$ is $f_{b_{\min}} = f_1/3 = 150$ mm; thus, according to Eq. (14), $\alpha \geq 60$. Thus our choice for α satisfies both cases.

The designed masks were done with a step of 0.04 in the fractional order p, starting from zero and ending in 0.96. Figure 3(a) illustrates the output obtained for the input of a Ronchi grating of 200 lines/cm. Figures 3(b) and 3(c) illustrate the output obtained for the input of a Ronchi grating of 100 and 50 lines/cm, respectively. Figures 4(a) and 4(b) illustrate the output plane for a chirp input,

$$\text{input} = \exp\left(-\frac{ix^2}{2f^2}\right)$$

with constants of $f = 1.5$ m and $f = 2.5$ m, respectively. Theoretically, it is known that the FRT of a chirp will be a δ function for the fractional order of

$$p = \frac{2}{\pi}\tan^{-1}\left(\frac{2\pi f^2}{\lambda f_1}\right), \tag{16}$$

and indeed in the experimental results a δ function (a bright dot) was obtained in the corresponding fractional order p.

Figure 5 demonstrates the output when a plane wave is used as input. Theoretically, the (x, p) of a plane wave should resemble a lying triangle with the edge of the triangle obtaining $p = 1$ (because the conventional Fourier transform of a constant is a δ function). The theoretically expected results were obtained in practice as can be seen from Fig. 5.

4. Conclusions

An optical setup for implementing the (x, p) display was suggested. The setup is relatively simple and requires only two masks. The masks consist of strips. Each strip is a different channel that performs an FRT with a different fractional order. The experimental output obtained suited the result anticipated from the theory. The display has several optical and digital applications. Optically it can describe the propagation of light through a GRIN medium, and digitally it can be used for classification and detection of linear FM components and in the noise reduction of multicomponent linear FM signals.

References

1. D. Mendlovic and H. M. Ozaktas, "Fractional Fourier transformations and their optical implementation: Part I," J. Opt. Soc. Am. A **10,** 1875–1881 (1993).
2. H. M. Ozaktas and D. Mendlovic, "Fractional Fourier transformations and their optical implementation: Part II," J. Opt. Soc. Am. A **10,** 2522–2531 (1993).
3. A. W. Lohmann, "Image rotation, Wigner rotation, and the fractional Fourier transform," J. Opt. Soc. Am. A **10,** 2181–2186 (1993).
4. D. Mendlovic, H. M. Ozaktas, and A. W. Lohmann, "Graded index fibers, Wigner distribution functions and the fractional Fourier transform," Appl. Opt. **33,** 6188–6193 (1994).
5. J. C. Wood and D. T. Barry, "Radon transform of the Wigner spectrum," in *Advanced Signal Processing Algorithms, Architectures, and Implementations III,* F. T. Luk, ed., Proc. SPIE **1770,** 358–375 (1992).
6. J. C. Wood and D. T. Barry, "Linear signal synthesis using the Radon–Wigner transform," IEEE Trans. Signal Process. **42,** 2105–2111 (1994).
7. J. C. Wood and D. T. Barry, "Tomographic time-frequency analysis and its application toward time-varying filtering and adaptive kernel design for multicomponent linear-FM signals," IEEE Trans. Signal Process. **42,** 2094–2104 (1994).
8. A. W. Lohmann and B. H. Soffer, "Relationships between the Radon–Wigner and fractional Fourier transforms," J. Opt. Soc. Am. A **11,** 1798–1801 (1994).
9. D. Mendlovic, Z. Zalevsky, R. G. Dorsch, Y. Bitran, A. W. Lohmann, and H. Ozaktas, "New signal representation based on the fractional Fourier transform: definitions," J. Opt. Soc. Am. A **12,** 2424–2431 (1995).
10. A. W. Lohmann, "A fake zoom lens for fractional Fourier experiments," Opt. Commun. (to be published).
11. H. M. Ozaktas and D. Mendlovic, "Multistage optical implementation architecture with least possible growth of system size," Opt. Lett. **18,** 296–298 (1993).
12. W. H. Lee, "Binary synthetic holograms," Appl. Opt. **13,** 1677–1682 (1974).